

Research Article

Finite Element Analysis of Magnetorheological Brake using ANSYS

Chiranjit Sarkar^{†*} and Harish Hirani[‡]

[†]Mechanical Engineering Department, Delhi Technological University, Shahbad Daluapur, Bawana Road, Delhi – 110042, India

[‡]Mechanical Engineering Department, Indian Institute of Technology Delhi, Hauz Khas, New Delhi – 110016, India

Accepted 06 March 2015, Available online 18 March 2015, Vol.5, No.2 (April 2015)

Abstract

The aim of this paper is to understand the electromagnetic action in a magnetorheological (MR) brake (MRB) system using finite element method. MR brake system consists of rotary disks immersed in a MR fluid and enclosed in an electromagnet. The torque exerted by MR fluid on the rotary disks is a function of magnetic field created by electric current passing through the electromagnet. To estimate the braking torque, under various operating conditions, an APDL code has been developed. Based on the parametric study, decisions on materials for various components of the MR brake have been made. Finally, a procedure to design a MR brake has been recommended.

Keywords: MR fluid, MR brake, Multi disk MR Brake, Electromagnetic simulation, Finite element analysis.

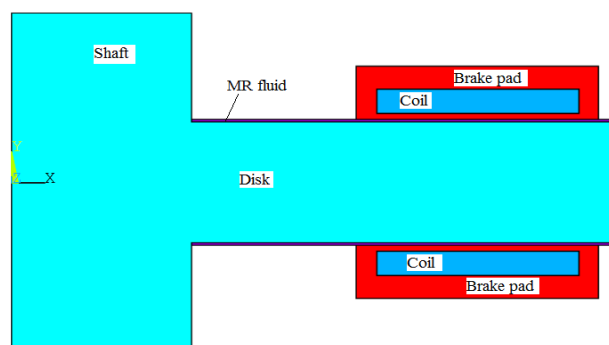
1. Introduction

In magnetorheological brake (Gupta and Hirani, 2011) torque can be magnetically manipulated by just controlling the electric current supplied to electromagnet. Such brake arrangement minimizes the number of moving links, reduces response time and increases the reliability of overall system. In addition, MR brake has advantage over conventional disk brakes, particularly in nullifying mechanical wear and providing digital control on the frictional power. It is expected that MR brake will perform smooth, jerk free operation and consume lesser power compared to eddy current or magnetic hysteresis brakes.

The design of MR brake starts with the maximum shear strength, τ_{max} , achievable by the available MR fluid (Ginder and Davis, 1994). The control on the shear stress (between zero to τ_{max}) of MR fluid is achieved by regulating the magnitude and direction of the magnetic field. The field density is a function of permeability and saturation of materials through which magnetic field passes, brake geometry, number of turns in electromagnetic coil, and current supplied to electromagnetic coil (Sarkar and Hirani, 2015), (Sarkar and Hirani, 2013), (Sukhwani, *et al*, 2009), (Sukhwani and Hirani, 2008), (Sukhwani and Hirani, 2008), (Sukhwani, *et al*, 2008), (Hirani and Manjunatha, 2007), (Sukhwani, *et al*, 2007), (Sukhwani and Hirani, 2007), (Sukhwani, *et al*, 2006). In the present study, magnetic flux density and flux path of magnetic field will be analyzed to understand the effect of magnetic and non magnetic materials using ANSYS software.

2. Electromagnetic simulation of MR brake

The geometry of MR brake is symmetric about the axis; therefore it is analysed as a 2-D axi-symmetric model as shown in Figure 1.



(a) Configuration 1



(b) Configuration 2

*Corresponding author: ChiranjitSarkar

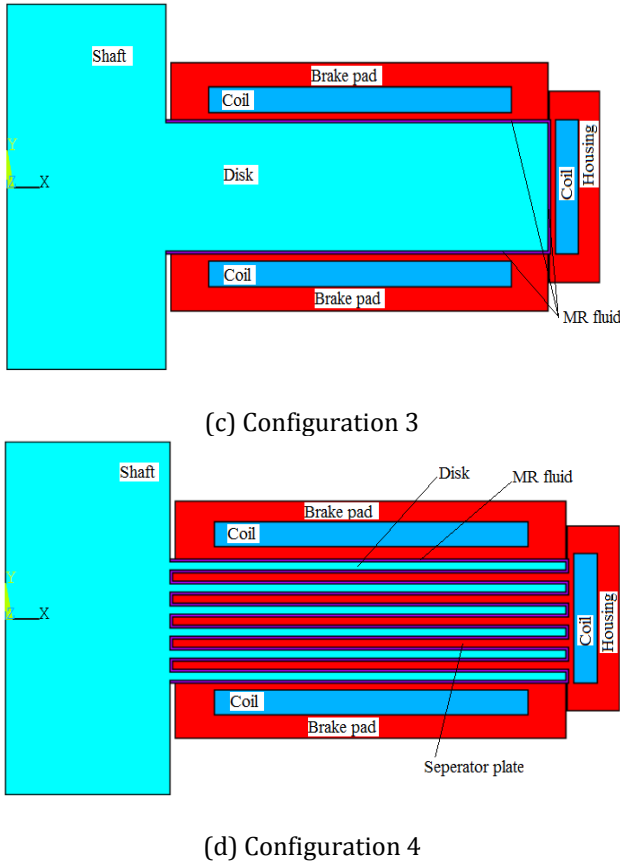


Fig.1 2-D Axisymmetric MR Brake in ANSYS

In Figure 1 (a) an axi-symmetric view of single disk MR brake has been shown. In this configuration it is assumed that rotating disk is mounted on the shaft with interference-fit and for FEA the shaft and rotating disk can be treated as a single component. Figure 1(b) is similar to Figure 1(a) except the changes in the brake-width and the coil area dimensions. In Figure 1 (c) additional electromagnetic coil pocketed in the housing has been shown. Figure 1 (d) shows a 2-D view of multi plate rotating disk attached to shaft and MR fluid around the rotating plates. Here brake pads and housing are stationary members. Three electromagnetic coils are shown in the figure. The details of the dimensions of four configurations are given in Sarkar and Hirani (2015). A cross sectional view of electromagnetic coil is shown in Figure 2.

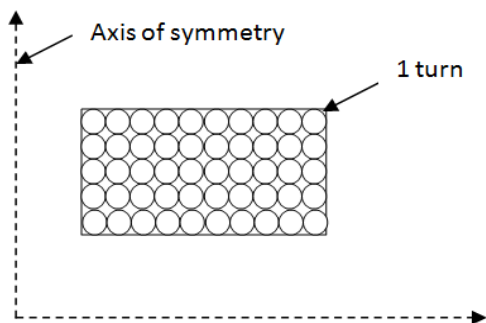


Fig.2 Axisymmetric cross section of electrical coil

For given current density, one can determine the magnetic flux density at the rotary disk, MR fluid and the housing. Table 1 lists the magnetic terms used in the present electromagnetic study of MR brake.

Table1: Nomenclature used for the Magnetic Analysis

Symbols	Meaning
BSUM	Magnetic Flux Density or Magnetic Induction
JS	Current Density
B	Vector Magnetic Flux Density
N	Numbers of turns of wires
I	Current
M	Permeability of material used in the Model

In ANSYS, a static (DC) current is provided as input in the form of current density (current over the area of the coil).

$$JS = \frac{(NI)}{A}$$

To mesh the geometry of MR brake, shown in Figure 1, 2-D quadrilateral Coupled-Field-Solid elements, PLANE 13 were selected. The PLANE 13 element contains four nodes and four degrees of freedom per node. The KEYOPT (3) option was selected to use axisymmetric simulation. The PLANE 13 element can be assigned nonlinear magnetic (B-H curves) properties. SI units were set using the EMUNIT command. The value of μ_0 (free-space permeability) was kept equal to $4\pi * 10^{-7}$ henries/meter. In ANSYS, the components of magnetic flux density along the x and y axes are nomenclature as B_x and B_y respectively. The term B_{Sum} is defined by

$$B_{Sum} = \sqrt{(B_x^2 + B_y^2)}$$

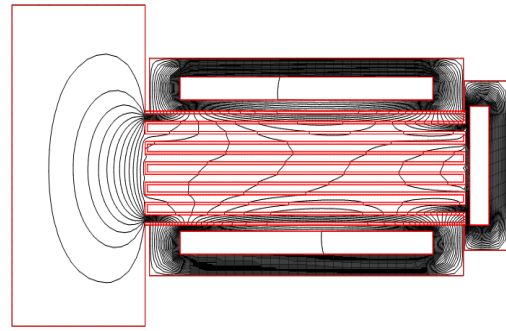
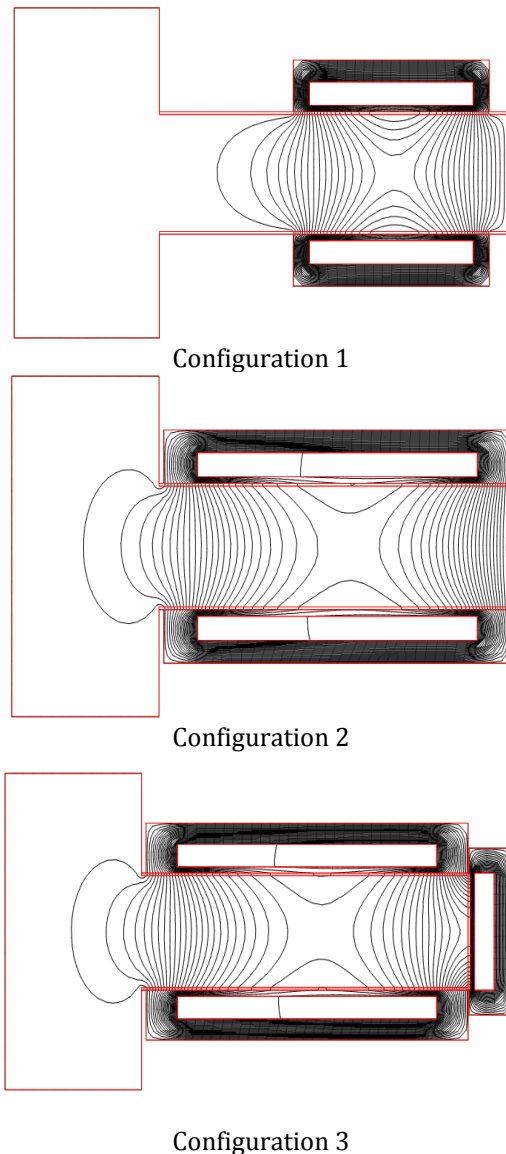
The values of relative permeability assigned to materials of various MR brake components are listed in Table 2. It shows MRF241ES (41% volume fraction of iron particles) and MRF336AG (36% volume fractions of iron particles) have relative permeability 8 and 5 respectively.

Table2: Relative permeability of different materials of the MR brake

Parts	Material	Relative Permeability
Shaft	Low carbon Steel/Stainless steel	100/1
Rotor plate	Low carbon steel/ Iron 99.8% pure	100/5000
Housing	Low carbon steel/ Iron 99.8 %pure	100/5000
Seals	Natural Rubber	1
Bearings	Low carbon steel/Stainless steel	100/1
MR fluid used	MRF 241 ES /MRF336AG	8/5

In the analysis an assumption of zero leakage from housing to the environment was made. To impose this condition, constraint of parallel direction of the magnetic flux on boundaries of housing ($AZ=0$) was used. By default, ANSYS uses the flux to be normal to all exterior faces. 2D magnetic static analysis (using MAGSOLV command) was performed to find the distribution of magnetic flux within the brake housing. To incorporate nonlinear B-H curve, nonlinear analysis (using NSUBST) was carried out. As nonlinear electromagnetic analysis proceeds, ANSYS computes convergence norms with corresponding convergence criteria in each equilibrium iteration. ANSYS considers a solution to be converged whenever specified convergence criteria are met. Convergence checking may be based on magnetic potential, magnetic field, or magnetic flux density. In the analysis, magnetic flux equal to 1.2 and the tolerance equal to 0.01 were selected, which means the convergence criterion for magnetic flux was kept as 0.012.

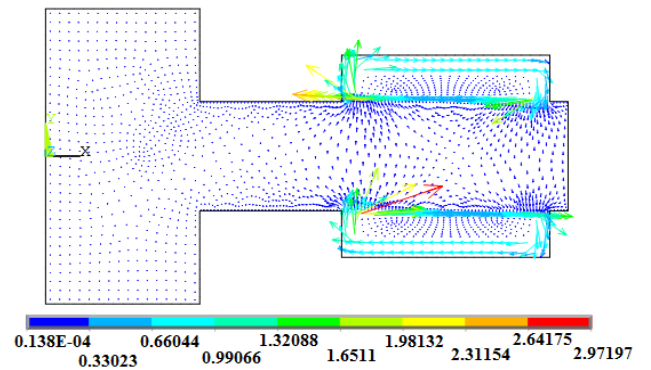
Figure 3 shows the flux lines of constant AZ (or constant radius-times-AZ for axisymmetric problems) for all four configurations.



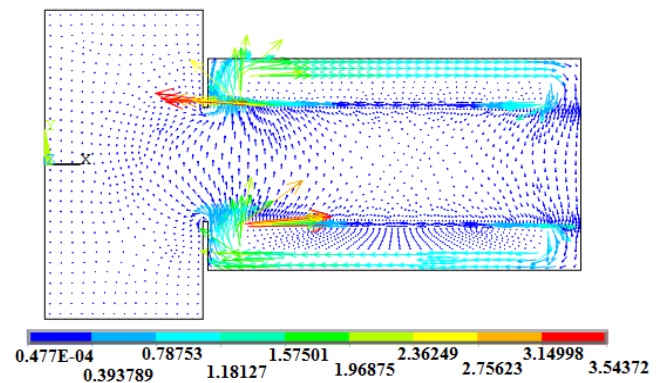
Configuration 4

Fig.32-D Flux Lines around the electrical coil

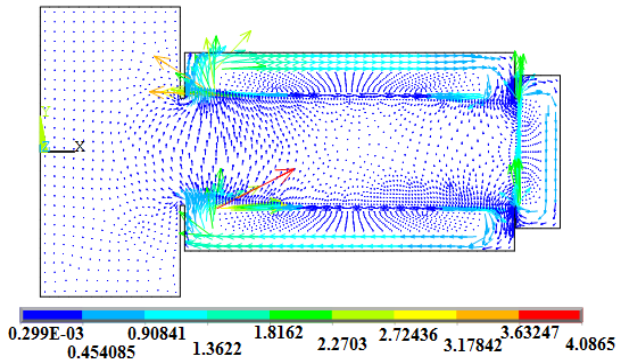
It shows that 2 D flux lines complete the path in the MR brake. The values of maximum density of 2 D flux lines (SMX) are 0.010702, 0.012923, 0.012967 and 0.012092 for configuration 1, configuration 2, configuration 3 and configuration 4 respectively. It indicates that with increase in the electromagnetic current density, maximum density of 2 D flux lines increases except in configuration 4. To justify the magnetic flux for different configurations, the vector plot of magnetic flux density using nodal solution has been plotted in Figure 4. It shows that configuration 3 has maximum magnetic flux density (SMX) of 4.08 Tesla. To observe the symmetrical magnetic flux density, $\frac{3}{4}$ expansion of the results for different configuration is shown in Figure 5. It shows the magnetic flux density is uniform along the circular direction.



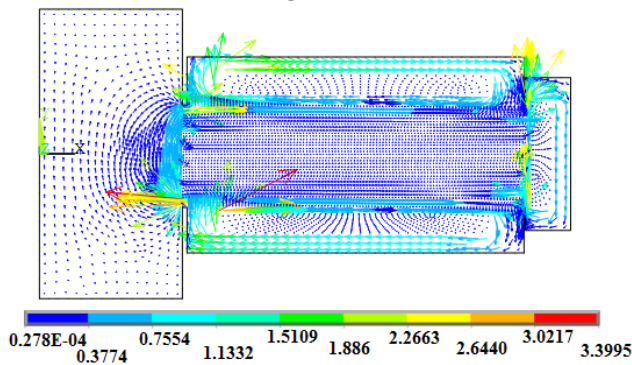
Configuration 1



Configuration 2

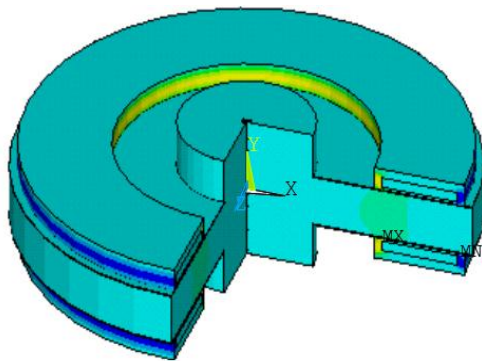


Configuration 3

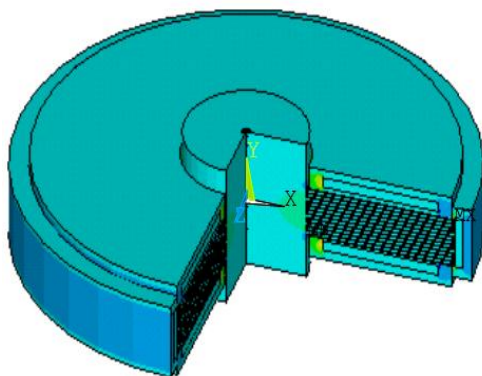


Configuration 4

Fig. 4 Nodal Solution-Magnetic Flux Density vector



Configuration 1



Configuration 4

Fig.5 3/4th Symmetry Expansion of MR Brake

This finite element analysis concludes that magnetic flux density is a function of radius of rotary disk. The magnetic flux densities at different nodes along the radius are different. To estimate the braking torque of MR brake, analysis of magnetic flux density at different nodes using APDL codes has been incorporated in the manuscript.

3. Estimating the Braking Torque using Finite Element Analysis

In this section, 2-D axi-symmetric analysis of a multi disk MR brake has been presented. Torque, exerted by the brake has been presented as function of MR gap and electric current supplied to electromagnet. APDL code was written for the finite element analysis.



Fig.6 Simple 2D Axisymmetric Model of MR Brake

A block axisymmetric model of multi disk is shown in figure 6. In this brake arrangement, MRF 336 AG is taken as MR fluid. The coil consists of 1000 turns of AWG 25 copper wire. The maximum current supplied to electromagnet was kept as 1 amp. The 2D flux lines of the multi disc brake assembly are illustrated in Figure 7.

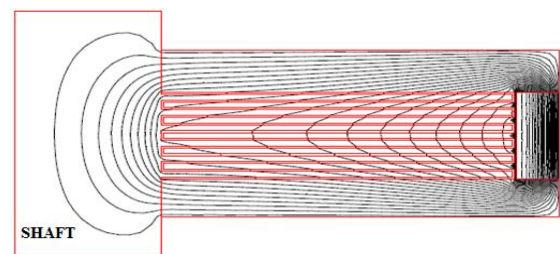


Fig.7 2D Flux Lines of multidisc assembly

It is interesting to note that flux lines are passing through the shaft. As torque is calculated along the disk, magnetic field concentration should be around the disk plate and magnetic field in the shaft should be as low as possible. Hence the shaft material should be non-magnetic material i.e. stainless steel.

Seals are required to restrict the leakage of the MR fluid. Seal is also made of non-magnetic material (i.e. Natural rubber) having permeability equal to 1. Bearing of permeability 1 is also placed to support the shaft. Figure 8 shows the multidisc assembly with the same sizes of seals and bearings.

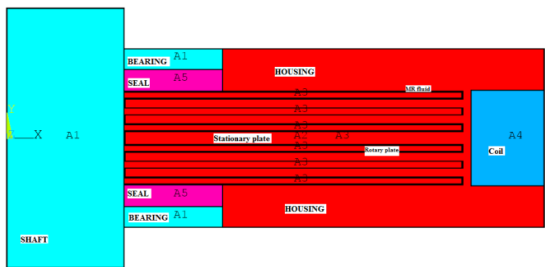


Fig.8 Modified design of Multi Disk assembly

Figure 9 shows the 2 D flux lines in the modified multi-disk brake assembly. It shows that negligible flux lines passes through the shaft, seal and bearing. Therefore, this design of MR brake is a good design as far as magnetic flux is concerned.

Figure 10 shows MR brake assembly with increase radial dimension of the disks, but maintaining overall same outer dimensions of the housing. This modification was attempted to increase the MR effect. Coil area is modified according to the number of turns of wire used.

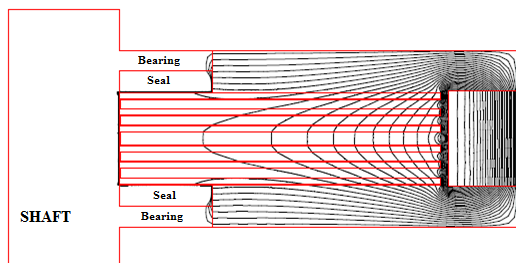


Fig.9 2 D Flux Lines of Modified Design of assembly



Fig.10 Modified MR Brake assembly

Figure 11 shows the 2D flux lines of the MR Brake assembly. It shows that the 2 D flux lines are more concentrated in the rotary plate of the disk which increases the magnetic flux density along the surface of the disk plate.

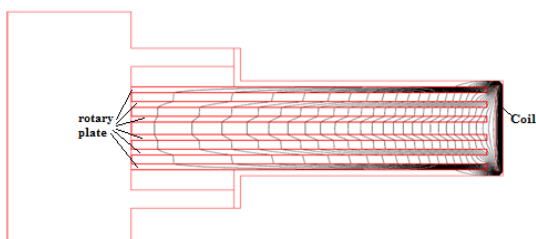


Fig.11 2D Flux Lines of MR Brake Assembly

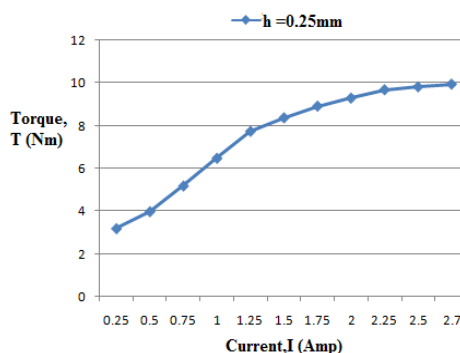
Torque of the modified MR brake assembly is estimated as function of MR gap ranging from 0.25mm to 1 mm. Rotary disk plates are made of silicone steel having relative permeability equal to 5000. The housing of MR brake is made low carbon steel having the relative permeability equal to 100. Coil is made copper wire (relative permeability = 0.999994). Table 3 shows the estimation of torque at different currents up to upper limit of current 2.7 Amp in AWG 25.

Table 3 shows the saturation of torque at the higher limit of current i.e. 2.5 A and 2.7 A. Figure 12 shows that torque increases with increase in h. Considering a constraint on outer radius of housing as 210 mm and packing factor as 0.7, a new electromagnet space was designed to accommodate the 2000 turns of wire to get more magnetic fields. Figure 13 shows the MR brake design with new electromagnet space. Figure 16 shows the torque of the MR brake using different housing materials.

Table 3: Estimation of torque at different currents

I (Amp)	Torque (Nm)			
	h = 0.25mm	h = 0.50mm	h = 0.75mm	h = 1.0 mm
0.25	3.17	5.44	7.69	9.86
0.5	3.97	7.11	10.26	13.25
0.75	5.17	9.30	13.64	17.79
1.0	6.47	11.93	17.80	22.65
1.25	7.73	14.84	22.49	29.37
1.5	8.36	16.85	26.20	34.39
1.75	8.91	18.46	28.29	38.14
2.0	9.29	19.67	30.22	41.41
2.25	9.68	20.87	32.37	44.89
2.5	9.81	21.26	34.64	46.72
2.7	9.94	21.78	35.52	47.43

There is a need to understand the material requirement for MR brake housing. Low permeability of material is required to minimize the leakage of magnetic field. However, higher permeability of material is required to transmit magnetic field from housing to rotating disks. To understand this, the simulation was carried on two materials: low carbon steel (relative permeability 100) and iron 99.8% pure as housing stationary plate (relative permeability 2000-5000). Table-4 indicates the torque-estimated for different housing material.



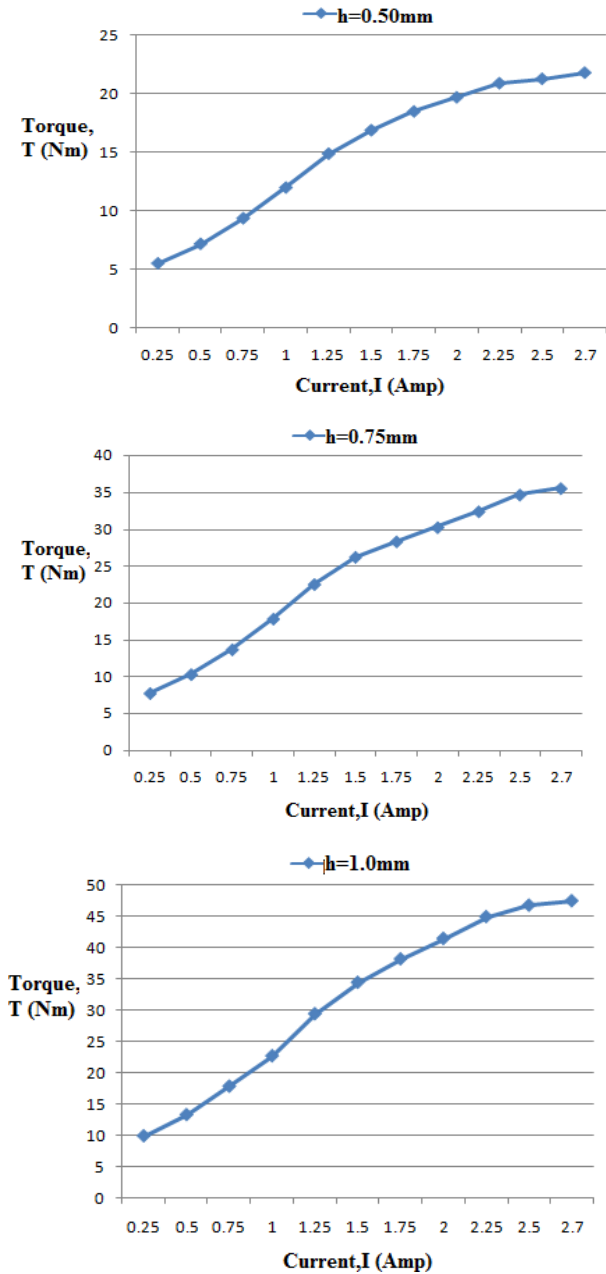


Fig.12 Torque at different MR gap, h

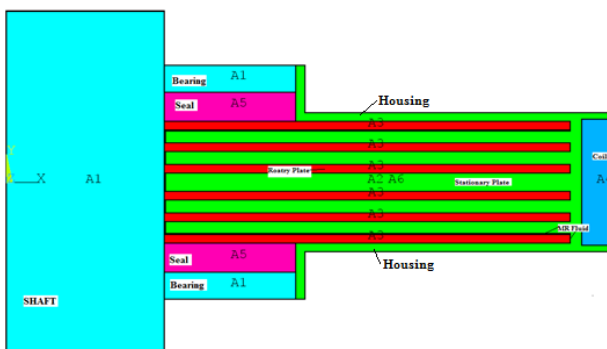
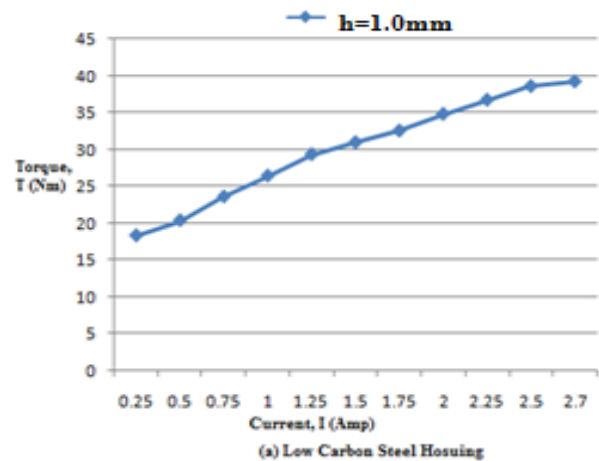


Fig.13 New design of multidisc MR brake

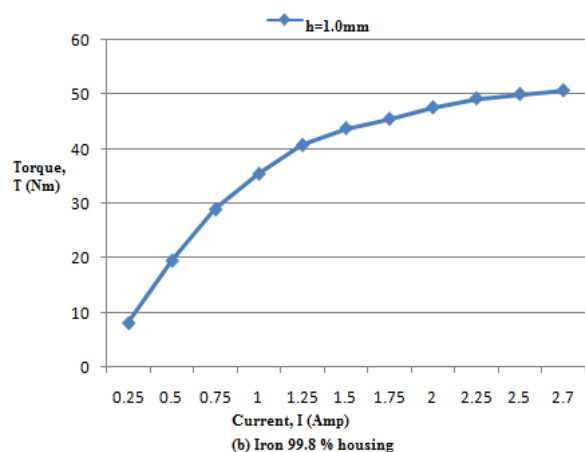
(Sarkar and Hirani, 2013). The maximum value of yield stress (τ_{yd}) corresponding to magnetic field intensity $H = 1000\text{kA/m}$ (Sarkar and Hirani, 2013), for the MRF 241 ES is 69 kPa (Sarkar and Hirani, 2013). Figure 16 shows the braking torque using MRF 241 ES MR fluid.

Table 4: Estimation of torque for different housing material

Current, I (Amp)	Torque at h = 0.001m	
	Low carbon steel Housing	Iron 99.8% Housing
0.25	18.32	8.16
0.5	20.37	19.57
0.75	23.58	28.96
1.00	26.41	35.46
1.25	29.33	40.73
1.5	30.93	43.80
1.75	32.51	45.52
2	34.78	47.60
2.25	36.69	49.27
2.5	38.56	50.06



(a) Low Carbon Steel Housing



(b) Iron 99.8 % housing

Fig.14 Effect of housing materials on the Braking Torque

Finally effect of MR fluid on brake was tried by using MRF 241 ES in place of MRF-336AG

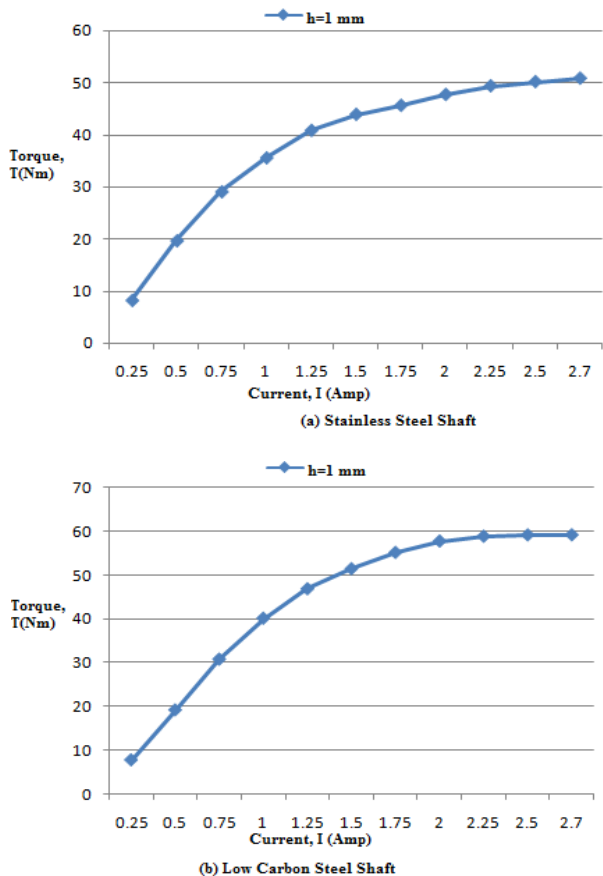


Fig. 15 Effect of shaft materials on the Braking torque

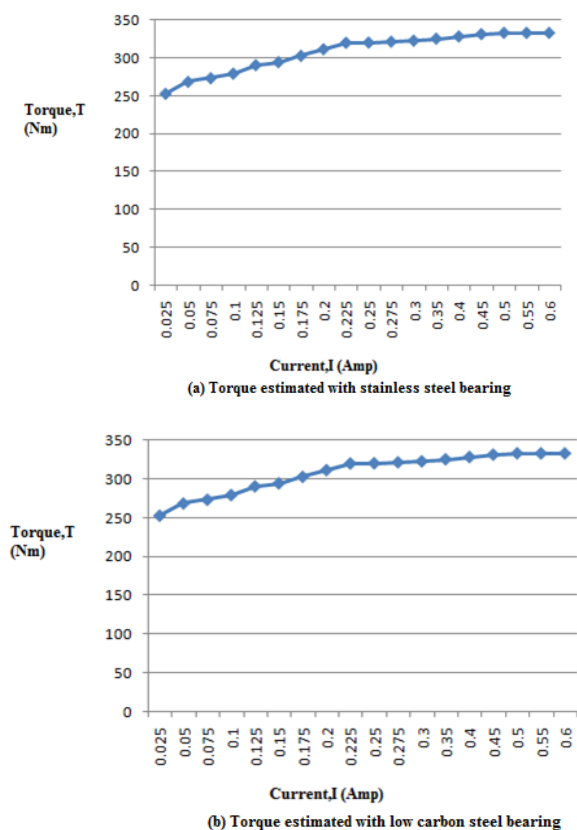


Fig.16 Torque estimated for MRF 241ES MR fluid

This figure clearly indicates that higher braking torque is possible by using MRF241 ES compared to using MRF 336 AG.

Conclusions

This research work has discussed the finite element analysis of the MR brake. The following conclusions can be made from the present research work.

- Density of 2 D flux lines in the MR brake configurations increases with increase in electromagnetic coil area.
- Non magnetic material seal (nitrile rubber) and bearing (stainless steel) restricts the passing of flux lines through them and enhances the concentrations of magnetic flux densities between disk, MR fluid and housing area. However, stainless steel bearing is costly.
- Increase in radial dimensions of the disk.
- With increase in MR gap, there is an increase in braking torque.
- Housing material with Iron 99.8% increases the braking torque as compared to Low carbon steel. Low carbon steel material of shaft increases MR effect as compared to stainless steel shaft.
- MRF241ES produces more braking torque due to high percentage of iron particles.

References

C.Sarkar, H.Hirani, (2013), Theoretical and experimental studies on a magnetorheological brake operating under compression plus shear mode, *Smart Materials and Structures*, 22, art. no. 115032.

C.Sarkar, H.Hirani, (2013), Synthesis and characterization of antifriction magnetorheological fluids for brake, *Defence Science Journal*, 63, pp. 408-412.

C.Sarkar, H. Hirani, (2013), Design of a squeeze film magnetorheological brake considering compression enhanced shear yield stress of magnetorheological fluid, *Journal of Physics: Conference Series*, 412, 012045.

C. Sarkar, H. Hirani, (2015), Transient Thermo Elastic Analysis of Disk Brake, *International Journal of Current Engineering and Technology*, 5, pp. 413-418.

C. Sarkar, H. Hirani, (2015), Magnetorheological Smart Automotive Engine Mount, *International Journal of Current Engineering and Technology*, 5, pp. 419-428.

C. Sarkar, H. Hirani, (2015), Design of Magnetorheological Brake using Parabolic Shaped Rotating Disc, *International Journal of Current Engineering and Technology*, 5, pp. 719-724.

C. Sarkar, H. Hirani, (2015), Synthesis and characterization of nano-copper-powder based magnetorheological fluids for brake, *International Journal of Scientific Engineering and Technology*, 4, pp. 76-82.

C. Sarkar, H. Hirani, (2015), Effect of particle size on shear stress of magnetorheological fluids, *Smart Science*, (in press).

C. Sarkar, H. Hirani, (2015), Development of magnetorheological brake with slotted disc, *Proc. IMechE, Part D: Journal of Automobile Engineering*, (in press).

H.Hirani, C. S. Manjunatha, (2007), Performance evaluation of magnetorheological fluid variable valve, *Proc. of the Institution of Mechanical Engineers, Part D, Journal of Automobile Engineering*, 221, pp. 83-93.

- J. M. Ginder, L. C. Davis, (1994), Shear Stresses in Magnetorheological fluids: Role of Magnetic Saturation, *Applied Physics Letters*, 65, pp. 3410-3412.
- S. Gupta, H. Hirani, (2011), Optimization of magnetorheological brake, *ASME/STLE 2011 International Joint Tribology Conference*, pp 405-406.
- V. K. Sukhwani, V. Lakshmi, H. Hirani, (2006), Performance evaluation of MR brake: an experimental study, *Indian Journal of Tribology*, pp. 67-52.
- V. K. Sukhwani, H. Hirani, T. Singh, (2007), Synthesis of magnetorheological grease, *Greasetech India*.
- V. K. Sukhwani, H. Hirani, (2007), Synthesis and characterization of low cost magnetorheological (MR) fluids, *The 14th International Symposium on: Smart Structures and Materials & Nondestructive Evaluation and Health Monitoring*, 65262R-65262R-12.
- V.K.Sukhwani, H.Hirani, (2008), A comparative study of magnetorheological-fluid-brake and magnetorheological-grease-brake, *Tribology Online*, 3, pp. 31-35.
- V.K.Sukhwani, H.Hirani, T.Singh, (2008), Synthesis and performance evaluation of MR grease, *NLGI Spokesman*, 71.
- V.K.Sukhwani, H. Hirani, (2008), Design, development and performance evaluation of high speed MR brake, *Proc. Institute Mech. Engineers., Part L, Journal of Materials: Design and Applications*, 222, pp.73-82.
- V. K. Sukhwani, H. Hirani, T. Singh, (2009), Performance evaluation of a magnetorheological grease brake, *Greasetech India*, 9, pp. 5-11.